ИНДЕКС 3649

ЕРЕВАНСКИЙ ФИЗИЧЕСКИЙ ИНСТИТУТ

Preprint YERPHI-1163(40)-89

ԵՐԵՎԱՆԻ ՖԻԶԻԿԱՅԻ ԻՆՍՏԻՏՈՒՏ
ЕРЕВАНСКИЙ ФИЗИЧЕСКИЙ ИНСТИТУТ
YEREVAN PHYSICS INSTITUTE

S.G.ARUTUNIAN, M.R.MAILIAN

TWELVE ILLUSTRATIONS OF THE SYNCHROTRON RADIATION FIELD

ЦНИИатоминформ
ЕРЕВАН - 1989

Նախնատիպ ԵՖԻ-1163(40)-89

Ս.Գ. ՀԱՐՈՒԹՅՈՒՆՅԱՆ, Մ.Ռ. ՍԱՑԱԿՅԱՆ

ՍԻՆՔՐՈՏՐՈՆԱՑԻՆ ՃԱՌԱԳԱՑՄԱՆ ԴԱՇՏԻ ՏԱՍՆԵՐԿՈՒ ՊԱՏԿԵՐՆԵՐ

Լորենց-կովարիանտ էլեկտրական դաշտի ուժագծերի օգնությամբ ստացվել են սինքրոտրոնային ճառագայթման դաշտի տարածական պատկերներ:

Երևանի ֆիզիկայի ինստիտուտ
Երևան 1989

Electromagnetic radiation is, as a rule, related to plane waves. Expansion of the synchrotron radiation in plane waves contains $\sim\gamma^3$ harmonics, where γ is the Lorentz-factor of charged particle. The characteristic length of radiation formation of $\sim R/\gamma$ is much shorter than R - the radius of the particles trajectory.

The use of Lienard-Wiechert formulae of field (see, e.g., ref.[1]) allows us, first, to follow the field formation from a Coulomb to a radiating one, second, to localize all the radiation harmonics in the space. As was expected, there appear fine spatial structures of field with characteristic sizes inversely proportional to the spectrum width (γ-regions). The force lines allow us to "visualize" the field [2]. As is shown in ref.[3], a successive introduction of systems of such lines allows one to rewrite in these terms the electrodynamics of orthogonal fields, including the Lienard-Wiechert one. There is constructed a system of force lines by which the charge field tensor is restored. In ref.[2] illustrations of the field lines in the orbit plane are presented.

In this paper spatial illustrations of the synchrotron radiation field of charges with Lorentz-factor γ=1.5 are obtained. The figures given allow us to present the field for large γ as well, including the characteristic values of electron accelerators.

1. The system of Lorentz-covariant field lines of a charge moving round a circle with radius R is written as:

$$\chi^{\mu}(\tau,\sigma;\, c_1,c_2) = R\{\sigma,\cos\beta\sigma + (\tau-\sigma)[\nu_1\cos\beta\sigma - \nu_2\sin\beta\sigma]\ ,$$

$$\sin\beta\sigma(\tau-\sigma)[\nu_1\sin\beta\sigma + \nu_2\cos\beta\sigma],\ (\tau-\sigma)\nu_3\}\ .$$

where

$$\nu_1 = \frac{\sqrt{1-c_2^2}\,\sin(\beta\gamma\sigma + c_1)}{\gamma(1+\beta\sqrt{1-c_2^2}\,\cos(\beta\gamma\sigma + c_1))},$$

$$\nu_2 = \frac{\beta + \sqrt{1-c_2^2}\,\cos(\beta\gamma\sigma + c_1)}{1+\beta\sqrt{1-c_2^2}\,\cos(\beta\gamma\sigma + c_1)},$$

$$\nu_3 = \frac{c_2}{\gamma(1+\beta\sqrt{1-c_2^2}\,\cos(\beta\gamma\sigma + c_1))}.$$

The z axis of the spatial coordinate system passes through the trajectory centre, perpendicular to its plane. $\tau=ct/R$ and $\sigma=ct'/R$ are the current and retarded times normalized to R/c. $\beta=(1-\gamma^{-2})^{1/2}$. At a fixed τ, variation of σ describes the magnetic field lines in a three-dimensional space. When c_1 varies within $0..2\pi$ and c_2 within $(-1..1)$, the lines (1) fill up the whole space. The surfaces c_2=const near the charge, form a system of cones one enclosed in another. The orbit plane corresponds to the condition $c_2=0$. Without loss of generality τ is taken equal to 0.

2. The synchrotron radiation electric field lines pattern in the orbit plane is presented, e.g., in ref.[2]. It is interesting to find out the behaviour of these lines out of the orbit plane.

In Fig.1 24 field lines on the surface $c_2=0.5$ are shown. But it is hard to realize these non-plane curves in a three-dimensional space by their two-dimensional image on the illustration plane. The lines pattern becomes visual when the unseen areas of the surface are removed. For this purpose a program of illustration of complicated two-dimensional surfaces has been written. We could not use the existing programs, because in this particular case the surface is not

clearly defined, but is given by the coordinates x,y,z as functions of σ and c_2. Reduction of such a dependence to the standard form z=f(x,y) requires solution of a great number of transcendental equations. It is convenient to use directly the formulae (1).

In further considerations the surfaces were projected at different angles θ and φ on a screen, where θ is the angle between the z axis and the screen plane, φ is the angle between the particle radius-vector at the moment of observation and the x_{sc} axis of the screen.

To separate the areas of the surface c_2=const seen and unseen on the display screen, it was scanned by the sections z=const or by the circles σ=const. At scanning the maximum value of the coordinate z_{sc}^{max} on the axis z_{sc}, which is normal to the screen and directed to the observer, was determined for each cell of the discrete screen grating (which is determined either by its resolution or can be purposely enlarged). By increasing the number of scanning lines and the points in them, we achieved a continuous image - each cell of projection had been scanned at least once. The data obtained (the values of z_{sc}^{max} in the corresponding cells) were written in a file. A section of the considered line between two successive points of its parameter, was displayed if at least one of the ends of that section satisfied the condition $|z_{sc}^{max} - z_{sc}^{l}|<EPS$, where z_{sc}^{l} is the z_{sc} coordinate on the line. The preliminary patterns were obtained at the same EPS for the whole surface. There is the following disadvantage connected with the fact that the surface c_2=const contains narrow regions of spatial localization of radiation with scale R/γ^3. To remove the unseen areas of such regions, we had to decrease EPS. On the other hand, at such parameters, the lines near the caustics of the surface c_2=const became discrete, where the normal to the surface was perpendicular to the z_{sc} axis. Decreasing of the parameter step along the line did not help, because some of its sections completely fell in the periphery of the corresponding screen cell, where

$|z_{sc}^{max} - z_{sc}^{l}| > EPS$.

To overcome these difficulties, EPS was varied as a function of the normal's inclination angle to the surface relative to the z_{sc} axis.

The normal to the surface, $\vec{n}_s$, was determined by the vector product of the tangent to the line displayed and the tangent to the lines σ=const (if scanning was performed by the levels z=const). The first tangent was defined numerically, and the second one - by the vector $\vec{n}_{c_1}$ which follows from (1):

$$\vec{n}_{c_1} = \frac{1}{\sqrt{1-c_2^2}} \{(\nu_z - \beta\gamma c_2 \nu_3)\cos\sigma + \nu_1 \sin\sigma \cdot$$

$$(\nu_z - \beta\gamma c_2 \nu_3)\sin\sigma - \nu_1 \cos\sigma \cdot \beta\gamma c_2 \nu_1\} \sim \quad (2)$$

EPS was substituted by:

$$EPS = EPS0\ (1+k\ \exp(-(\vec{n}_s z_{sc})^2/(EPS1)^2)) \cdot \quad (3)$$

The parameters EPS0, k, EPS1 were chosen empirically. Near the caustic ($|\vec{n}_s z_{sc}| < EPS1$) the sign of the product $\vec{n}_s z_{sc}$ was additionally checked and the areas for which it became negative were not displayed regardless the results of comparison of z_{sc}^{max} with z_{sc}^{l}.

The proposed algorithm turned out to be convenient also when illustrating surfaces one enclosed in another, which correspond to different values of c_2. As much as possible values of $z_{sc,i}^{max}$ from the files corresponding to different c_2 (denoted by the index i) were compared for each screen cell. The thus obtained information about the combined surface points nearest to the obzerver, was written in a new file and then was used to illustrate the field lines.

The results of the work of programs are shown in Figs 1-12. γ=1.5 for all the patterns. With the Lorentz-factor

increasing, the characteristic "arms" of the γ-regions become knife-like.

The illustrations of the electric field lines (Figs 1,2,4,5,6,7,8,9,10), the levels z=const (Fig.3) and the lines σ=const (Figs 11,12) are presented. In Figs 5 and 9 the electric field lines in the orbit plane are also shown. Surfaces one enclosed another and corresponding to different values of c_2, are also illustrated (Figs 9 and 10).

For clearness the z axis in Figs 3-12 is scaled up twice.

There is seen a definite progress in Figs 2-12 as compared to Fig.1, where the field lines are shown without removing the unseen areas.

More detailed explanations are given in figure captions.

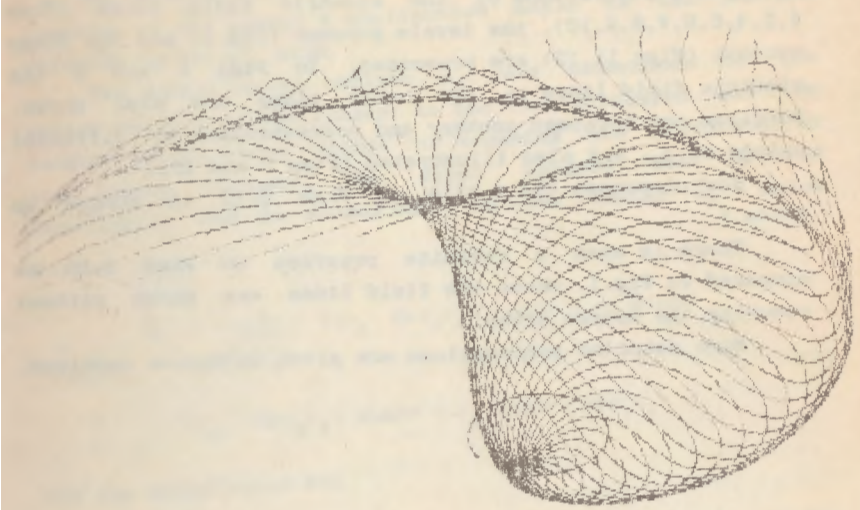

Fig.1 Illustrations of electric field lines on the surface c_z=0.5 . The angles θ and φ are equal to $7\pi/24$ and $19\pi/32$. respectively. The particle trajectory is marked by an arrow. A field created by a particle moving along the local section of the trajectory shown in the figure is considered for clearness. Intersection of the projections of different sections of lines on the figure's plane makes it difficult to present the surface on which they lie. One also fails to follow the behaviour of the field lines.

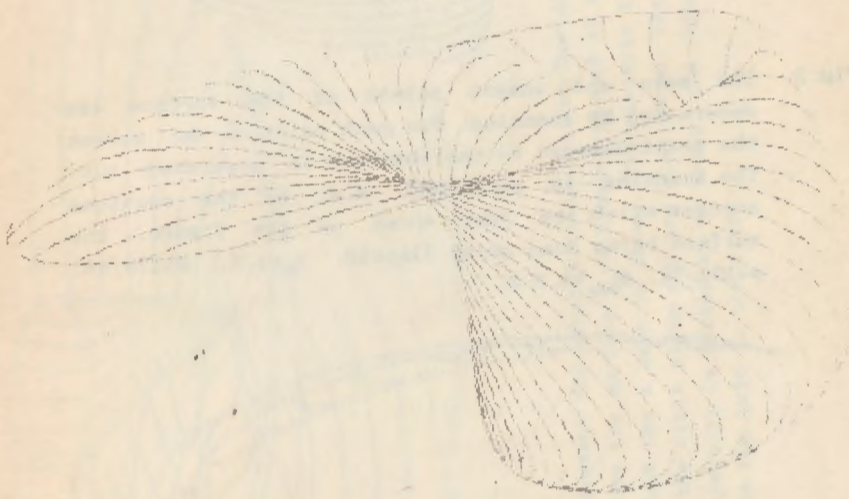

Fig 2 To show the surface formed by the field lines. it is necessary to stretch an opaque film on the carcass formed by these lines and remove the areas which are not seen at projection on the figure's plane. Comparison with Fig.1 reveals the advantage of removal of the unseen points of the surface (θ and φ are the same).

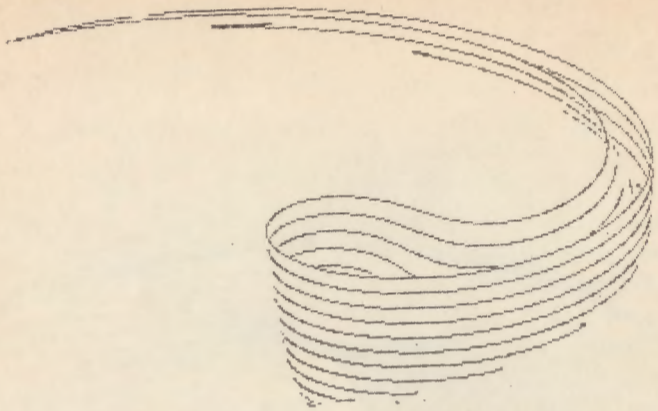

Fig.3 The seen and unseen points of the surface are determined by scanning. For each point on the screen the point nearest to the observer is separated out. The scanning is performed, e.g. by the sections z=const which are just shown in the figure, the surface being seen quite clearly. c_z=0.5, $\theta=17\pi/48$, $\varphi=19\pi/32$, z_{max}=1.5 R.

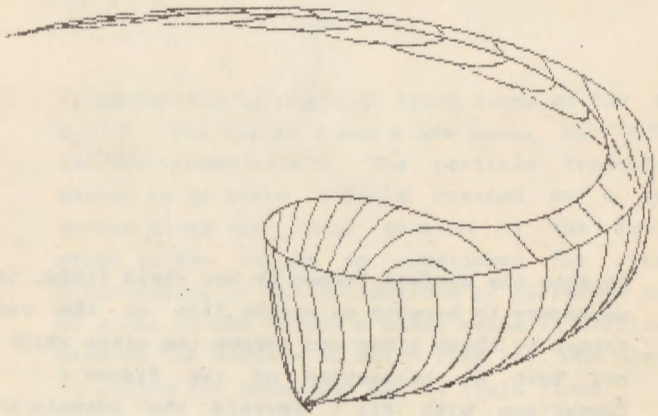

Fig.4 Now on the surface c_z=0.5 one can draw electric field lines, cutting them off at z=1.5 R. The characteristic bent "arm" is the γ-region. Here the fields are most intensive.

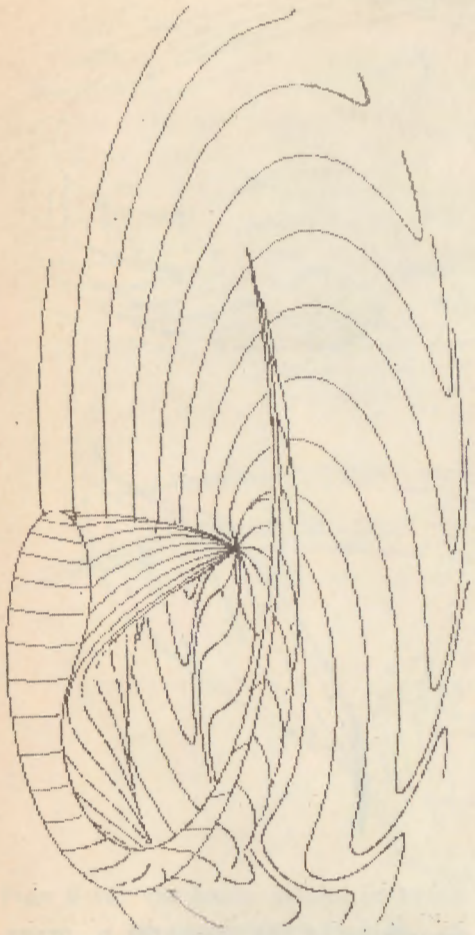

Fig.5 To present the general field pattern better, in this figure the surface c_z=0.5 being turned at an angle π around the z axis is shown. The electric field lines in the orbit plane z=0 are also shown. The particles trajectory is marked by an arrow, the charge moving from the left to the right.

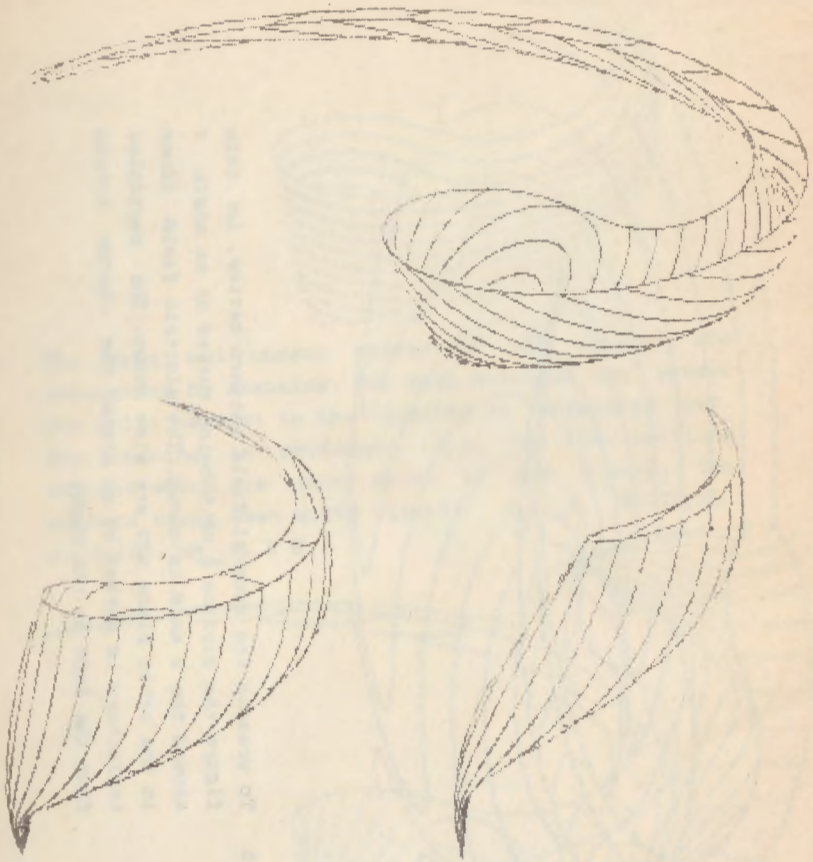

Figs 6-8 Remember, that decreasing of the parameter c_2 draws the surfaces c_2=const nearer to the orbit plane, and its increasing makes them narrower and more extended. θ and φ are the same. In Fig.6 c_2=0.3, z_{max}=1.0 R; in Fig.7 c_2=0.8, z_{max}=2.2 r; in Fig.8 c_2=0.95, z_{max}=2.7 R.

Figs 9-10 The whole system of field lines in the space can be represented as a set of field-line systems on surfaces one enclosed in another. Near the charge it is a system of cones one enclosed in another, on which straight field lines are lying. In Figs 9.10 the surfaces from Figs 4 and 6 and 4.6-8, respectively, are enclosed one in the other.

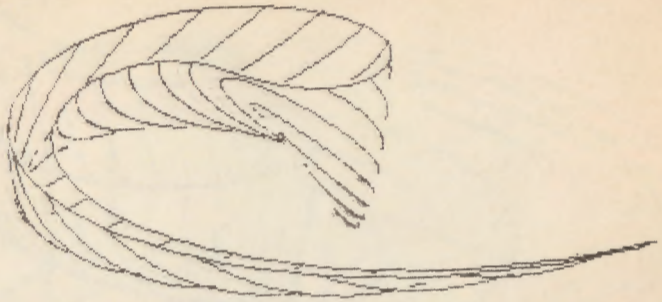

Figs 11-12 It is interesting that the surfaces c_z=const are formed by circles corresponding to σ=const and to the variation of c_z from 0 to π. Such circles are shown for the surfaces c_z=0.5. z_{max}=1.5 R (Fig.11) and c_z=0.8. z_{max}=2.2 R (Fig.12).

References

1. Арутюнян С.Г., Нагорный П.А. Эффекты интенсивности в ускорителях и накопителях, связанные с линейно-поляризованными полями частиц. Препринт ЕрФИ-453(30)-80. Ереван. 1980.
2. Арутюнян С.Г. Линии электромагнитного поля продольно движущейся в вакууме точечной заряженной частицы. УФН. 1986. 150. 3. 445-452.
3. Arutunian S.G., Saltuffian M.M. Orthogonal Fields Electrodynamics and Dynamics of Force Lines. Preprint YERPHI-991(41)-87. Yerevan. 1987.
4. Котов Ю.Б. Как рисует машина. М., Наука. 1988.
5. Харп Д., Бейер М. Инженерная графика. М., Мир. 1987.

The manuscript was received May 11, 1989

С.Г. АРУТЮНЯН, М.Р. МАИЛЯН
ДВЕНАДЦАТЬ ИЛЛЮСТРАЦИЙ ПОЛЯ МАГНИТНО-ТОРМОЗНОГО ИЗЛУЧЕНИЯ

(на английском языке, перевод Г.А. Папяна)
Редактор Л.П.Мукаян
Технический редактор А.С.Абрамян

Подписано в печать 27/9/89г. ВФ-02109 Формат 60×84×16
Офсетная печать. Уч.изд.л., 1,0 Тираж 299 экз.Ц.15 к.
Зак.тип. 1589 Индекс 3649

Отпечатано в Ереванском физическом институте
Ереван-36, ул. Братьев Алиханян 2.